PROCEEDINGS, Twenty-Second Workshop on Geothermal Reservoir Engineering
Stanford University, Stanford, California, January 27-29, 1997
SGP-TR-I55

IN-SITU STRESS IN A FA JLT-HOSTED GEOTHERMAL RESERVOIR AT DIXIE VALLEY, NEVADA

Stephen Hickman' and Mark Zoback[2]

[1]U.S. Geological Survey
345 Middlefield Road
Menlo Park, CA 94025, U.S.A
hickman@thepub.wr.usgs.gov

*Departmentof Geophysics
Stanford University
Stanford, CA 94305, U.S.A
zoback@pangea.stanford.edu

ABSTRACT

As part of a study relating fractured rock hydrology to in-situ stress and recent deformation within the Dixie Valley Geothermal Field, borehole televiewer logging and hydraulic fracturing stress measurements were conducted in a 2.7-km-deep geothermal production well (73B-7) drilled into the Stillwater fault zone. The borehole televiewer logs from well 73B-7 show numerous drilling-induced tensile fractures, indicating that the direction of the minimum horizontal principal stress, S_{hmin}, is S57°E ± 10°. As the Stillwater fault at this location dips S50°E at ~53°, it is nearly at the optimal orientation for normal faulting in the current stress field. Analysis of the hydraulic fracturing data shows that the magnitude of S_{hmin} is 24.1 and 25.9 MPa at 1.7 and 2.5 km, respectively. Analysis of a hydraulic fracturing test from a shallow water well (24W-5) 1.5 km northeast of 73B-7 indicates that the magnitude of S_{hmin} is 5.6 MPa at 0.4 km depth. Given the calculated vertical stress, Coulomb failure analysis indicates that the magnitude of S_{hmin} measured in these wells is close to that predicted for incipient normal faulting on the Stillwater and other subparallel faults, using laboratory-derived coefficients of friction of 0.6 to 1.0 and estimates of the in-situ formation fluid pressure.

INTRODUCTION

Although relatively few fractures and faults *can* control fluid flow in low-porosity crystalline rock, the reasons why some fractures and faults are much more permeable than others are poorly known [*see* Long et al., 1996]. Understanding the origins and characteristics of these fractures and faults **requires** analysis of the local fracture and fault systems in the context of the current stress field and tectonic history. The primary objective of this study is to define the nature, distribution and hydraulic properties of fractures controlling fluid flow within a commercial geothermal reservoir at Dixie Valley, Nevada, and to characterize the manner in which these fractures, and hence the overall reservoir hydrology, are related to the in-situ stress field.

The Dixie Valley Geothermal Field (DVGF) is located in the western Basin and Range province **of** west-central Nevada (Figure 1). This area is characterized by active seismicity, high heat flow and late Cenozoic extensional faulting and volcanism. The DVGF is coincident with the moderately (52-54°) dipping, roughly northeast-striking Stillwater fault zone — a major, active, range-bounding normal fault exhibiting a total displacement of about 3 km [Okaya and Thompson, 19851. The Stillwater fault zone is associated with extensive fracturing and recent hydrothermal alteration [e.g., Parry et al., 19911 and comprises the dominant reservoir for a –62 MW geothermal electric power plant operated by Oxbow Geothermal Corporation. Although earthquakes have not ruptured this segment of the Stillwater fault in historic times, large (M = 6.8-7.3) earthquakes have occurred within the past 80 years along range-bounding faults –20 km to the northeast and southwest of the DVGF (Figure 1) and geologic evidence shows that the Stillwater fault abutting the DVGF experienced two **or** more faulting episodes (total offset –9 m) during the past 12,000 years [Wallace and Whitney, 1984].

In this study, hydraulic fracturing stress measurements were conducted in a 2.7-km-deep geothermal production well (well 73B-7) drilled into the Stillwater fault zone in late 1995 by Oxbow Geothermal Corporation (Figure 1). This well was drilled to within 2° of the vertical from the surface to a depth **of** 1.98 km, where it was intentionally deviated in a S60°W direction to intersect the

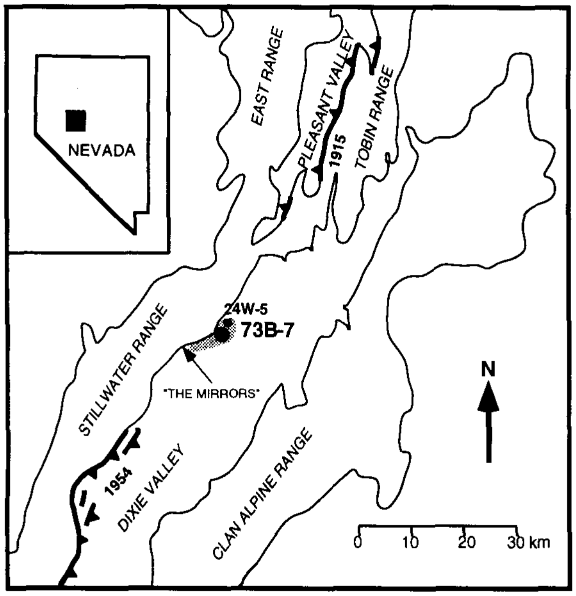

Geothermal Field (shaded area) and wells 73B-7 and 24W-5. Surface ruptures of the 1915 and 1954 normal faulting earthquakes are shown as heavy lines (M = 7.3 and 6.8, respectively). The southeast-dipping Stillwater fault zone, which was intersected by well 73B-7 at about 2.7 km depth, forms the eastern boundary of the Stillwater Range. Also shown is the location of a surface outcrop of the Stillwater fault zone at the "Mirrors".

Stillwater fault zone. We also acquired borehole televiewer, spinner flowmeter and high-resolution temperature logs from this well. Interpretation of these logs for fracture orientation, permeability and permeability anisotropy is discussed by Barton et al. [this issue]. Below, results are presented from the hydraulic fracturing tests in well 73B-7 together with stress directions inferred from observations of borehole wall tensile failure. Results are also presented from a hydraulic fracturing stress measurement conducted in January 1997 in a ~0.6-km-deep water well (well 24W-5) located approximately 1.5 km northeast of well 73B-7 (Figure 1).

The ultimate objective of these investigations is to obtain a comprehensive suite of thermal, hydrologic and stress data from widely spaced wells within and adjacent to the DVGF. By comparing and contrasting data from both productive and non-productive wells, it should be possible to determine if a relationship exists between the contemporary in-situ stress field and reservoir productivity. These data should allow one to determine if it is possible to predict which faults or fault segments are likely **to** be hydraulically conductive in a given stress field, and to provide input on decisions related to redrilling of wells or

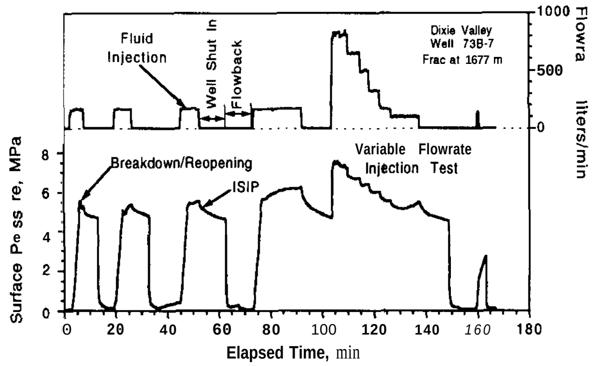

Figure 2: Surface pressure and flowrate records from the hydraulic fracturing test conducted at 1663-1690 m depth in well 73B-7. Pressures were also recorded during each test using a downhole temperature-compensated quartz pressure transducer suspended a few meters above the test interval.

abandonment **of** an area or prospect. At some future date it is hoped these methods can be used to locate and engineer future production and injection wells and to design enhanced recovery programs (e.g., massive hydraulic fracturing) for less-than-commercial wells within existing geothermal reservoirs.

METHOD

The hydraulic fracturing technique and the interpretation methods used at Dixie Valley are described in detail elsewhere [Hickman and Zoback, 19831. Although hydraulic fracturing tests are typically conducted in short (1- to 3–m–long) intervals of open hole using inflatable rubber packers, high borehole temperatures precluded the use **of** packers in well 73B-7. Instead, following cementation and pressure testing of the casing at two different depths in this well, 15- to 30-m-long pilot holes were drilled out the bottom of the well and the entire casing string was pressurized to induce a hydraulic fracture in the uncased pilot hole. Repeated pressurization cycles were then employed to extend this fracture away from the borehole. Pressures and flowrates were measured at the surface. In addition, a high-accuracy, temperature compensated **quartz** pressure gauge was suspended about 10 m above the test interval to provide a continuous record of downhole pressure during each test. The magnitude of the least horizontal principal stress, S_{hmin}, was determined from the instantaneous shut-in pressure (ISIP), or the pressure at which the pressure-time curve departs from an initial linear pressure drop immediately after the pump is turned off and the well is shut in (Figure 2). Furthermore, downhole pumping pressures measured during a stepwise change in **flow** rate in the last pumping cycle of each test were used to detect changes in the apparent permeability of the test interval resulting from

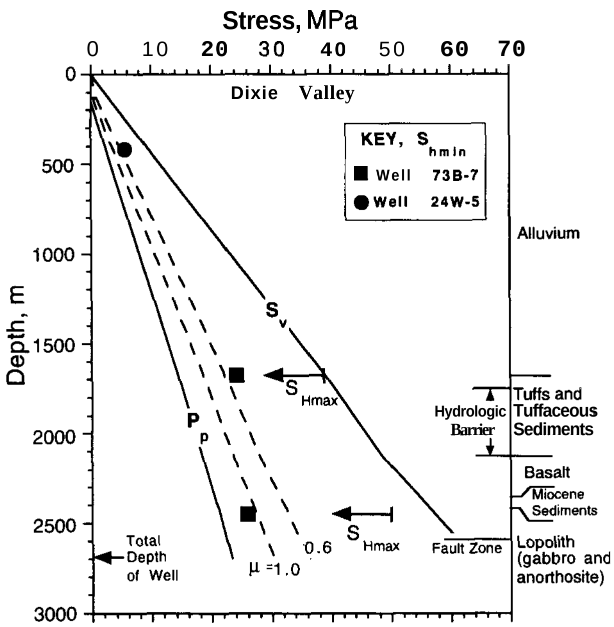

Figure 3. Magnitude of the least horizontal principal stress, S_{hmin}, from the two deep hydraulic fracturing tests in well 73B-7 and a shallow test in well 24W-5. Also shown are upper bounds on the magnitude of the greatest horizontal principal stress, S_{Hmax}, based upon the absence of stress-induced borehole breakouts in well 73B-7. The vertical stress, S,, and the pore fluid pressure, P_p, were calculated for the appropriate densities. The dashed lines indicate the range of S_{hmin} at which incipient normal faulting would be expected on optimally oriented faults for coefficients of friction of 0.6 to 1.0.

closure of the hydraulic fracture close to the borehole. The pressure at which this change occurred provided an additional constraint on the magnitude of S_{hmin} that agreed closely with the value determined from the minimum **ISIP** recorded during each test.

In a hydraulic fracturing test the magnitude of the maximum horizontal principal stress, S_{Hmax}, is typically determined utilizing a fracture initiation, or breakdown, criteria derived for fractures initiating in intact rock at the optimal orientation for tensile failure (i.e., pure Mode **I). In** well 73B-7, however, borehole televiewer logs [see Barton et al., this issue] conducted before and after the hydraulic fracturing tests showed that the tested intervals contained numerous pre-existing fractures at a variety of orientations. Thus, it was not possible to directly measure the magnitude of S_{Hmax} during these tests. However, following Moos and Zoback [1990], upper bounds to the magnitude of S_{Hmax} were obtained using estimates **of** the compressive strength of rock types encountered in this well [from Lockner 1995] and the absence of borehole breakouts in the borehole televiewer logs from this well.

The vertical (overburden) stress, **S,,** was calculated using geophysical density logs conducted in nearby wells in conjunction with rock densities measured on hand samples obtained from surface outcrops at Dixie Valley [Okaya and Thompson, 1985].

RESULTS AND DISCUSSION

Two hydraulic fracturing tests were conducted in well 73B-7, covering the depth intervals from 1663–1690 m and 2439–2455 m. The shallowest test was conducted across the transition from the alluvial valley fill to the underlying tuffs, whereas the deepest test was conducted in the gabbro and anorthosite lopolith, about 150 m above the shallowest geothermal production zone encountered in this well. Analysis of these **data** shows that the magnitude of S_{hmin} is 24.1 ± 0.6 and 25.9 ± 0.5 MPa at 1.68 **and** 2.45 km, respectively (Figure 3). The observation that the magnitude of S_{Hmax}, as derived from the breakout analysis described above, is less than S_v indicates a normal faulting stress regime. The procedure for the shallow hydraulic fracturing test in well 24W-5 was similar to that used in 73B-7, with the exception that a drill-pipe-deployed packer was employed to isolate the open-hole interval (i.e., from 400–550 m) from the casing during pressurization and a spinner log was run during the final cycle of the test to identify the depth of the induced hydraulic fracture. This test indicates that the magnitude of S_{hmin} at a depth of 412 m is 5.6 ± 0.5 MPa (Figure 3).

Information on stress orientations was provided by the borehole televiewer log from well 73B-7. These televiewer images show numerous long, subvertical, undulatory cracks that are roughly parallel to the borehole and occur on diametrically opposed sides of the hole. As discussed by Moos and Zoback [1990}, these cracks result from the superposition of a tensional circumferential thermal stress induced by circulation of relatively cold drilling fluids and the concentration of ambient (i.e., tectonic) stresses at the borehole wall. **As** these tensile cracks should form along the azimuth of maximum applied compressive stress, they indicate that the direction of S_{Hmax} in this well is **N33°E** ± 10° (Figure **4).** The corresponding S_{hmin} direction is nearly perpendicular to the local strike **of** the Stillwater fault (Figure *5)* and is in very good agreement with other stress-direction indicators in the western Basin and Range [Zoback, 19891.

In conducting this analysis, only those tensile fractures from the vertical portion of well 73B-7 were used (i.e., above 2 km in Figure 4). This approach was adopted for two reasons. First, the orientations

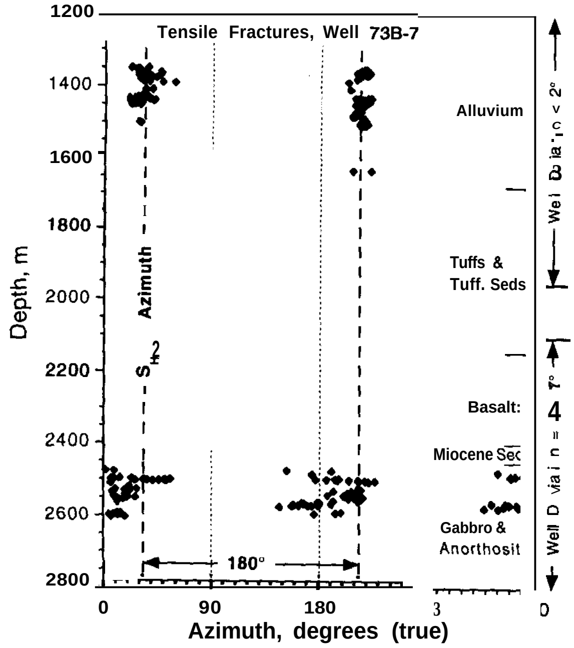

Figure 4. Azimuth of borehole wall tensile cracks observed in the borehole televiewer log from well 73B-7. As described in the text, tensile cracks from the portion of the borehole that was within 2" of vertical (see range of deviations along right-hand margin) were used to determine that the azimuth of the maximum horizontal compressive stress, S_{Hmax}, at this site is N 33" E ± 10°.

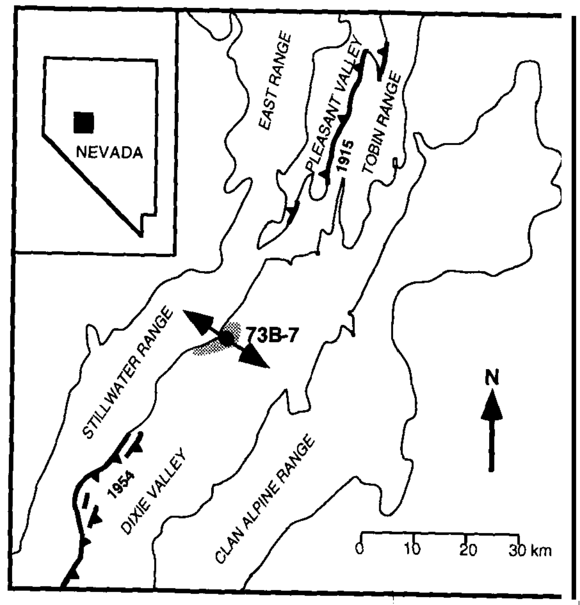

Figure 5. Same as Figure 1, but showing t orientation of the least horizontal principal stre S_{hmin}, as determined from tensile cracks in well 73B (outward-pointing arrows).

of tensile fractures at greater depths were observed to change by several tens of degrees over short depth intervals (e.g., at 2505 m in Figure 4). As discussed by Barton and Zoback [1994], these rotations suggest localized perturbations to the regional stress field, perhaps due to slip on nearby permeable faults and fractures associated with the Stillwater fault zone [see Barton et al., this volume]. Second, depending upon the relative magnitudes of the two horizontal principal stresses, the large deviation of the borehole from the vertical below 2 km could lead to significant differences between the azimuth of tensile cracks at the borehole wall and the far-field S_{Hmax} direction [e.g., Peska and Zoback, 19951.

Since the S_{hmin} azimuth determined in this well indicates that the Stillwater fault is nearly at the optimal orientation for normal faulting, the stress magnitudes from the hydraulic fracturing tests can be analyzed in terms of the potential for slip on this and other (subparallel) faults. In accordance with the Coulomb failure criterion, frictional sliding will occur on optimally oriented faults at a critical ratio of the maximum and minimum effective principal stresses (i.e., the principal stresses minus the pore pressure). If these planes have zero cohesion, then in a normal faulting regime sliding would occur at a critical magnitude of S_{hmin}, given by [Jaeger a Cook, 1976, pp. 97, 223]:

$$S_{hmin\ crit} = (S_v - P_p) / [(\mu^2 + 1)^{1/2} + \mu]^2 + P_p \quad (1)$$

where P_p is the pore fluid pressure and μ is the coefficient of friction of preexisting faults. We assume here that μ ranges from 0.6 to 1.0, in accord with laboratory sliding experiments [after Byerlee, 19781. Estimates of undisturbed (i.e., pre-production) formation fluid pressure were obtained assuming that P_p was in hydrostatic equilibrium with the water table at 152 m depth by integrating water density as a function of pressure and temperature (from Keenan *et al.*, 1978), as appropriate to ambient geothermal conditions, and including a small correction for total dissolved solids. Pressure logs conducted in deep (≤ 2.7 km) wells drilled into the Stillwater fault zone and adjacent rocks prior to large-scale geothermal production about 10 years ago indicate that this P_p is accurate to within 0.5 MPa for units penetrated by well 73B-7, at least below about 200–300 meters. Since that time, however, geothermal production has drawn the water table in aquifers deeper than about 2 km (i.e., beneath the hypothesized hydrologic barrier shown in Figure 3) down from its original level of 152 m to a depth of about 600 m.

Using equation (1), the range of S_{hmin} magnitudes at which normal faulting would be expected can be calculated given the calculated vertical stress (Figure 3). This analysis indicates that S_{hmin} at 0.4 and 1.7

km is close to that predicted by frictional faulting theory for incipient normal faulting on the Stillwater fault, using laboratory-derived coefficients of friction and estimates of the in-situ pore pressure that existed prior to reservoir production. The magnitude of S_{hmin} at 2.4 km, however, is somewhat lower than expected based upon this simple failure model. This reduction in the magnitude of S_{hmin} at depth might be a consequence of geothermal production, perhaps through a combination of poroelastic effects associated with a decrease in reservoir pressure (e.g., Segall *et al.,* 1994) and thermal stresses due to heat extraction, coupled with an increase in fault strength due to decreased fluid pressure. Alternatively, the larger differential stress **(S,** - S_{hmin}) indicated at 2.4 km depth may suggest that solution-transport processes such as crack healing, crack sealing and cementation have acted to generate slight cohesive strength along the Stillwater fault at depth. This inference is in general accord with surface observations of mineral deposition and crack healing associated with the Stillwater fault zone [e.g., Parry et al., 1991; Seront *et al.,* 19971. It is important to note, however, that laboratory tests conducted on samples from the core of the Stillwater fault zone recovered from a nearby surface outcrop (the "Mirrors", see Figure 1) indicate strengths comparable to those predicted by Byerlee's Law [Seront *et al.,* 19971.

Analysis of hydraulic fracturing stress measurements at the Nevada Test Site in the southern Basin and Range similarly indicate incipient normal faulting, with sub-hydrostaticfluid pressures and coefficients of friction of 0.6–1.0 [Stock et al., 19851. In contrast to well 73B-7, however, the magnitude of S_{hmin} at the Nevada Test Site, at least at shallow depths (0.5–1.5 km), was found to be less than the fluid pressure in the borehole when it was filled to the surface, resulting in serious lost circulation problems during drilling [Stock et al., 1985]. In-situ stress measurements at both sites, however, indicate that slip along nearby active normal faults occurs at high levels **of** resolved shear stress — in **accord** with "strong-fault'' models derived from simple interpretations of laboratory experiments. This is in marked contrast to stress field indicators and heat-flow measurements indicating that the San *Andreas* fault, and perhaps many other plate-boundary faults as well, is quite weak and sliding at low levels of resolved shear stress [e.g., Lachenbruch and Sass, 1980; Zoback et al., 1987; see review by Hickman, 19911.

Although the causes for the relative weakness of the San *Andreas* fault are unknown, numerous possibilities have been suggested – including intrinsically low coefficients of friction, elevated fluid pressures, transient weakening associated with earthquake rupture propagation, and solution-transport deformation (e.g., pressure solution). In this regard, it is noteworthy that this segment of the Stillwater fault appears capable of producing large-magnitude earthquakes and, based upon microstructural studies ***of*** exhumed fault rocks at the Mirrors locality (Figure 1), may deform in the interseismic period through a pressure-solution-type mechanism even at relatively shallow depths (i.e., < 2 km and < 270° C; Power and Tullis, 1989). **If** these inferences are correct, then the observation that the Stillwater behaves as a "strong" fault suggests that neither the dynamics ***of*** earthquake rupture propagation nor pressure solution necessarily lead to weak-fault behavior at mid- to upper-crustal conditions.

SUMMARY

Hydraulic fracturing stress measurements and observations of borehole wall tensile failure to ~3 km depth in Dixie Valley wells 73B-7 and 24W-5 indicate that in-situ stresses are of the appropriate magnitude and orientation for frictional failure (i.e., normal faulting) on the Stillwater and nearby sub-parallel faults. The determined magnitude **of** the least horizontal principal stress, S_{hmin}, is in accord with simple frictional faulting theory for a "strong" fault — i.e., assuming laboratory-derived coefficients of friction of 0.6–1.0 and hydrostatic fluid pressures. The magnitude **of** S_{hmin} measured near the bottom **of** well 73B-7, however, departs somewhat from a failure law assuming slip on pre-existing cohesionless faults, suggesting that hydrothermal processes might have acted to restrengthen the Stillwater and associated faults at depth since the last major slip episode. This information is important for developing a conceptual model for tectonic controls on permeability and permeability anisotropy in the Dixie Valley Geothermal Field. Results from this project may also be important in understanding the coupling between fluid flow and faulting in other fault-hosted geothermal reservoirs.

REFERENCES

Barton, C.A. and M.D. Zoback (1994), ":Stress Perturbations Associated with Active Faults Penetrated by Boreholes: Possible Evidence for Near-Complete Stress Drop and a New Technique for Stress Magnitude Measurements", *Journal of Geophysical Research,* **99,** 9373-9390.

Byerlee, **J.** (1978), "Friction of Rocks", Pure and Applied Geophysics., **116,** 615-626.

Hickman, S.H., and M.D. Zoback (1983), 'The Interpretation of Hydraulic Fracturing Pressure-time Data for In-situ Stress Determination", in Hydraulic Fracturing Measurements, M.D. Zoback and B.C. Haimson (eds.), National Academy Press, Washington, D.C., 44-54.

Hickman, **S.** (1991), "Stress in the Lithosphere and the Strength of Active Faults", U.S. National Report to the International Union of Geodesy and Geophysics 1987--1990, Reviews of Geophysics Supplement, April 1991, 759-775.

Jaeger, J.C., and N.G.W Cook (1976), "Fundamentals of Roch Mechanics", 2nd ed., 585 pp., Chapman and Hall, London.

Keenan, J.H., F.G. Keyes, P.G. Hill, and J.G. Moore (1978). *Steam Tables: Thermodynamic Properties of Water Including Vapor, Liquid, and Solid Phases.* John Wiley & Sons, New York, 156. pp.

Lachenbruch, A. H., and J. H. Sass (1980), "Heat Flow and Energetics **of** the San Andreas Fault Zone", Journal of Geophysical Research, ***85,*** 6185-6222, 1980.

Lockner, D.A. (1995), "Rock Failure", in Rock Physics and Phase Relations: A Handbook of Physical Constants, T. Ahrens (ed.), American Geophysical Union, Washington, D.C., 127-147.

Long, J.C., et al. (1996), (Committee on Fracture Characterization and Fluid Flow, **U.S.** National Committee **for** Rock Mechanics), "Rock Fractures and Fluid Flow: Contemporary Understanding and Applications", National Academy Press, Washington, D.C., 551 pp.

Moos, D., and M.D. Zoback (1990), "Utilization of Observations of Well Bore Failure to Constrain the Orientation and Magnitude **of** Crustal Stresses: Application to Continental, Deep Sea Drilling Project, and Ocean Drilling Program Boreholes", Journal of Geophysical Research, 95,9305-9325.

Okaya, D.A., and G. Thompson (1985), "Geometry of Cenozoic Extensional Faulting: Dixie, Valley, Nevada", Tectonics, 4, 107-125.

Parry, W.T., D. Hedderly-Smith, and R.L. Bruhn (1991), "Fluid Inclusions and Hydrothermal Alteration on the Dixie Valley Fault, Nevada", Journal of Geophysical Research, 96, 19733-19748.

Peska, P., and M.D. Zoback (1995), "Observations of Borehole Breakouts and Tensile Wall Fractures in Deviated Boreholes: A Technique to Constrain In Situ Stress and Rock Strength", Journal of Geophysical Research, **100,** 12791-12811.

Power, W.L., anf T.E. Tullis (1989), "The Relation between Slickenside Surfaces in Fine-Grained Quartz and the Seismic Cycle", *Journal of Structural Geology,* **11,** 879-893.

Segall, P., J.R. Grasso, and A. Mossop (1994), "Poroelastic Stressing and Induced Seismicity Near the Lacq Gas Field, Southwestern France", Journal **of** Geophysical Research, 99, 15423-15438.

Seront, B., T.-F. Wong, J.S. Caine, C.B. Forster, and J.T. Fredrich (1997), "Laboratory Characterization **of** Hydromechanical Properties **of** a Seismiogenic Normal Fault System", *Journal of Structural Geology* (in press).

Stock, J. M., J. H. Healy, **S.** H. Hickman, and M. D. Zoback (1985), "Hydraulic Fracturing Stress Measurements at Yucca Mountain, Nevada, **and** Relationship to the Regional Stress Field", Journal of Geophysical Research, 90, 8691-8706.

Wallace, **R.E.,** and R.A. Whitney (1984), "Late Quaternary History of the Stillwater Seismic Gap, Nevada", Bulletin of the Seismological Society of America, 74, 301-314.

Zoback, M. D., M. L. Zoback, **V. S.** Mount, J. Suppe, J. P. Eaton, J. H. Healy, D. Oppenheimer, P. Reasenberg, L. Jones, C. B. Raleigh, I. G. Wong, **O.** Scotti, and C. Wentworth (1987), "New Evidence on the State of Stress of the San Andreas Fault System", Science, **238,** 1105-1111.

Zoback, M. L. (1989), "State of Stress and Modem Deformation **of** the Northern Basin and Range Province", Journal of Geophysical Research, 94, 7105-7128.